Supplementary material

for

Adenosine-to-inosine *Alu* RNA editing controls the stability of the pro-inflammatory long noncoding RNA *NEAT1* in atherosclerotic cardiovascular disease

Nikolaos I. Vlachogiannis[1,2,*], Marco Sachse[1,3*], Georgios Georgiopoulos[4], Eleftherios Zormpas[1], Dimitrios Bampatsias[4], Dimitrios Delialis[4], Francesca Bonini[1,3], George Galyfos[5], Fragiska Sigala[5], Kimon Stamatelopoulos[4], Aikaterini Gatsiou[1,†] and Konstantinos Stellos[1-3,†]

[1]Biosciences Institute, Vascular Biology and Medicine Theme, Faculty of Medical Sciences, Newcastle University, Newcastle Upon Tyne, UK.

[2]Department of Cardiology, Freeman Hospital, Newcastle Hospitals NHS Foundation Trust, Newcastle upon Tyne, UK.

[3]Vascular Inflammation and RNA Metabolism Laboratory, Institute for Vascular Signalling, JW Goethe University Frankfurt, Frankfurt am Main, Germany.

[4]Department of Clinical Therapeutics, Alexandra Hospital, National and Kapodistrian University of Athens, Athens, Greece.

[5]First Propaedeutic Department of Surgery, National and Kapodistrian University of Athens, Hippocration Hospital, Athens, Greece.

* Equal first authorship

† Equal last authorship and co-correspondence.

Correspondence shall be addressed to: Aikaterini Gatsiou, PhD; or Konstantinos Stellos, MD; Biosciences Institute, Faculty of Medical Sciences, Newcastle University, International Centre for Life, Central Parkway, Newcastle Upon Tyne NE1 3BZ, United Kingdom. Telephone: +44(0) 191 241 8629, Fax: +44 191 241 8666. Email: aikaterini.gatsiou@ncl.ac.uk or konstantinos.stellos@ncl.ac.uk

File content:

Supplementary Table 1: Descriptive baseline characteristics of study cohort.

Supplementary Table 2: Sequences of siRNAs used in the study.

Supplementary Table 3: Sequences of primers used in the study.

Supplementary Table 4: Predictors of *NEAT1* expression in PBMCs

Supplementary Figure 1: Distribution of *NEAT1* expression levels across *NEAT1* tertiles.

Supplementary Figure 2. NEAT1 lncRNA expression levels in PBMCs of male vs female individuals.

Supplementary Figure 3. *NEAT1* lncRNA expression in dose-dependent TNF-α treatment of HUVECs.

Supplementary Figure 4. Efficiency of NEAT1 knockdown in endothelial cells.

Supplementary Figure 5: Supportive documentation of the dsRNA foldback analysis and the RNA editing studies.

Supplementary Figure 6: Supportive documentation of the ARE sites mapping on the secondary *AluSx3*$^{+}$ and *AluJo*$^{-}$ dsRNA foldback structure of *NEAT1*.

Supplementary Table 1. Descriptive baseline characteristics of the study cohort

	Study cohort (n=153)	**non-est. CVD individuals (n=105)**	**CAD (n=48)**	**P-value***
Age[years], median(IQR)	64 (17)	60.0 (19)	69 (13)	<0.001
Sex[male], n(%)	86 (56.6)	43 (41.3)	43 (89.6)	<0.001
BMI[kg/m^2], median(IQR)	26.8 (5.3)	26.9 (5.9)	26.7 (4.4)	0.601
Smoking, n(%)	41 (27.3)	26 (25.0)	15 (32.6)	0.427
Arterial hypertension, n(%)	84 (56.0)	44 (42.3)	40 (87.0)	<0.001
Hyperlipidemia, n(%)	93 (62.8)	53 (52.0)	40 (87.0)	<0.001
Family history of CAD, n(%)	41 (27.5)	27 (26.0)	14 (31.1)	0.552
Type 2 diabetes mellitus, n(%)	36 (24.0)	17 (16.3)	19 (41.3)	0.002
SBP[mmHg], mean(SD)	131 (22)	127 (19)	143 (25)	<0.001
DBP[mmHg], mean(SD)	72 (11)	71 (11)	74 (12)	0.269
Creatinine[mg/dl], median(IQR)	0.85 (0.61)	0.73 (0.45)	1.13 (0.77)	<0.001
hsCRP[mg/L], median(IQR)	1.52 (2.93)	1.2 (2.3)	2.33 (7.26)	0.011
eGFR[ml/min/1.73m^2], mean(SD)	80.3 (36.7)	86.9 (35.5)	64.8 (35.2)	0.001
Medications at admission				
Aspirin, n(%)	37 (24.8)	5 (4.8)	32 (71.1)	<0.001
Statins, n(%)	70 (47.0)	36 (34.6)	34 (75.6)	<0.001
RAAS-inhibitors, n(%)	53 (35.6)	25 (24.0)	28 (62.2)	<0.001
Beta-blockers, n(%)	46 (30.9)	19 (18.3)	27 (60.0)	<0.001
Calcium channel blockers, n(%)	37 (24.8)	19 (18.3)	18 (40.0)	0.007

*P-value represents the comparison between non-est. CVD individuals and CAD patients.

Continuous variables are presented as mean (SD) or median (IQR) when non-normally distributed. P-value is derived from independent samples t-test or Mann-Whitney U test, respectively.

Categorical variables are presented as absolute count (valid percentage) and P-values are derived from Fisher's exact test.

Abbreviations: *non-est. CVD*: non-established cardiovascular disease; *BMI*: body mass index; *CAD*: coronary artery disease; *SBP*: systolic blood pressure; *DBP*: diastolic blood pressure; *hsCRP*: high-sensitivity C-reactive protein; *eGFR*: estimated glomerular filtration rate; *RAAS*: renin-angiotensin-aldosterone system

Supplementary Table 2. Sequences of siRNAs used in the study.

Name	siRNA sequence (5' - 3')	
scrambled siRNA	UCUCUCACAACGGGCAUUU(dT)(dT)	Sigma-Aldrich
siADAR1	GCUAUUUGCUGUCGUGUGA(dT)(dT)	Sigma-Aldrich
siELAVL1	GGCUUGAGGCUCCAGUCAA(dT)(dT)	Sigma-Aldrich
siAUF1	GAAGGUGAUUGAUCCUAAA(dT)(dT)	Sigma-Aldrich
siPOOL neg. control	n/a	siTOOLs Biotech
siPOOL *NEAT1*.2	n/a	siTOOLs Biotech

Supplementary Table 3. Sequences of primers used in the study.

Name	Forward primer (5' - 3')	Reverse primer (5' - 3')
RPLP0	TCGACAATGGCAGCATCTAC	ATCCGTCTCCACAGACAAGG
ADAR1	TGCTGCTGAATTCAAGTTGG	CCCCAACTTTTGCTTGGTAA
NEAT1 long	GGCCAGAGCTTTGTTGCTTC	GGTGCGGGCACTTACTTACT
HuR (ELAVL1)	GAAGACCACATGGCCGAAGA	CCAAGCTGTGTCCTGCTACT
AUF1 (HNRNPD)	CACAGCGGGAAGAATGGAAAA	TGGCTTTGGCCCTTTTAGGA
NEAT1 AluJo^{-}	GCCCAGTAACCCTGGAAGAAC	GTTCCCAACCCTCTGCACTG
NEAT1 AluSx3^{+}	GTGGTCAGGGAAGGTAACCC	ATCCTACCCAAAACCTGCCTG

Supplementary Table 4. Determinants of *NEAT1* expression in PBMCs

	Univariable		Adjusted for presence of CAD	
	OR (95% CI)	**P-value**	**Adjusted OR (95% CI)***	**Adjusted P-value**
Male sex	2.16 (1.18-3.93)	0.012	1.25 (0.64 – 2.44)	0.515
Arterial hypertension	1.80 (0.99-3.27)	0.053	1.04 (0.53 – 2.03)	0.908
Aspirin	4.40 (2.09-9.29)	<0.001	2.12 (0.76 – 5.93)	0.151
Calcium channel blockers	2.28 (1.12–4.64)	0.022	1.73 (0.83-3.60)	0.141
Presence of CAD	4.43 (2.24-8.78)	<0.001	n/a	n/a

Odds ratio was calculated using ordinal logistic regression with NEAT1 tertiles as dependent variable.

Supplementary Figure 1

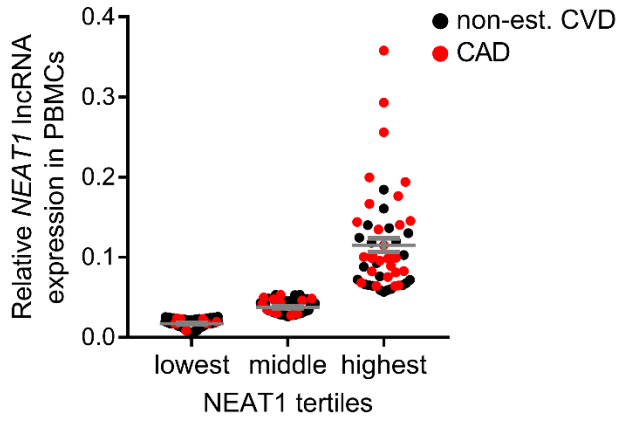

Supplementary Figure 1. Distribution of *NEAT1* expression levels across *NEAT1* tertiles. Dot plots represent individual *NEAT1* lncRNA expression levels in PBMCs in the lowest (n=51), middle (n=51) and highest (n=51) *NEAT1* tertile. Black dots represent non-established CVD individuals (controls, n=105), while red dots represent patients with CAD (n=48). Lines represent mean±SEM per tertile. SEM: standard error mean.

Supplementary Figure 2

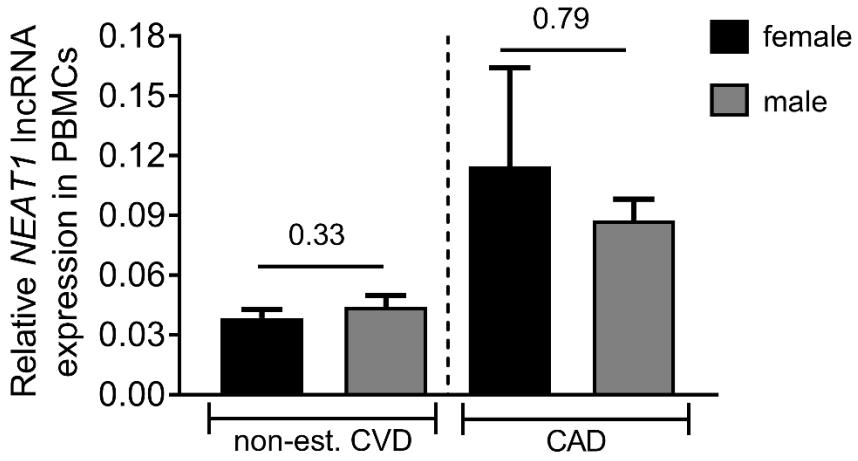

Supplementary Figure 2. NEAT1 lncRNA expression levels in PBMCs of male vs female individuals. *NEAT1* lncRNA expression in PBMCs of male *vs* female individuals without established CVD (non-est. CVD) and in CAD patients. Bar-graphs represent mean+SEM. SEM: standard error mean.

Supplementary Figure 3

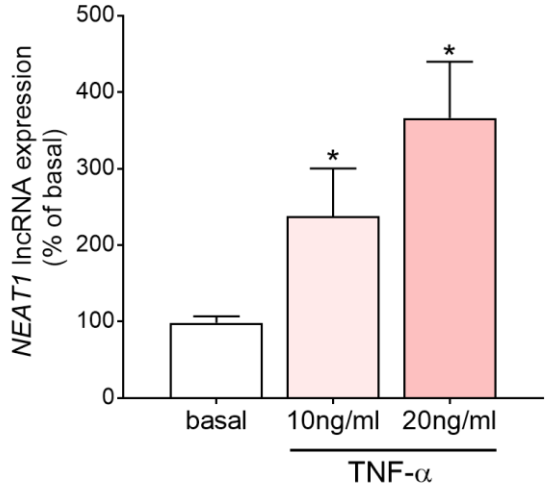

Supplementary Figure 3. NEAT1 lncRNA expression in dose-dependent TNF-α treatment of HUVECs. P<0.05 *vs* basal for all using Mann Whitney *U* test. One-way ANOVA analysis followed by multiple comparisons Dunnett's correction statistical test showed that *NEAT1* lncRNA expression remained significantly increased only after 20 ng/ml TNF-α treatment (P=0.015 *vs* basal).

Supplementary Figure 4

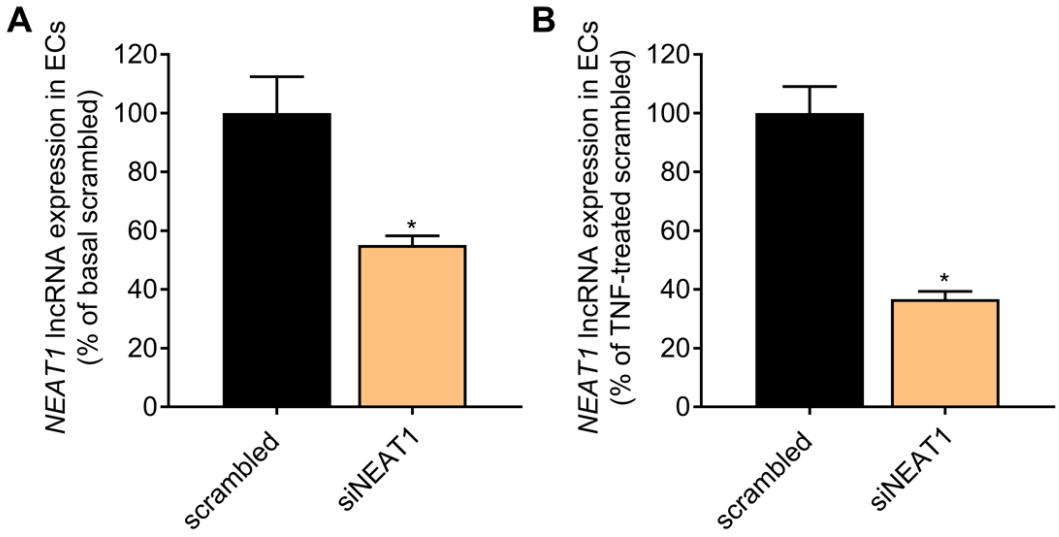

Supplementary Figure 4. Efficiency of NEAT1 knockdown in endothelial cells. *NEAT1* lncRNA expression in scrambled- vs siNEAT1-transfected endothelial cells. Bar-graphs represent mean+SEM derived from 4 independent biological replicates. SEM: standard error mean *****P<0.05 vs scrambled.

Supplementary Figure 5

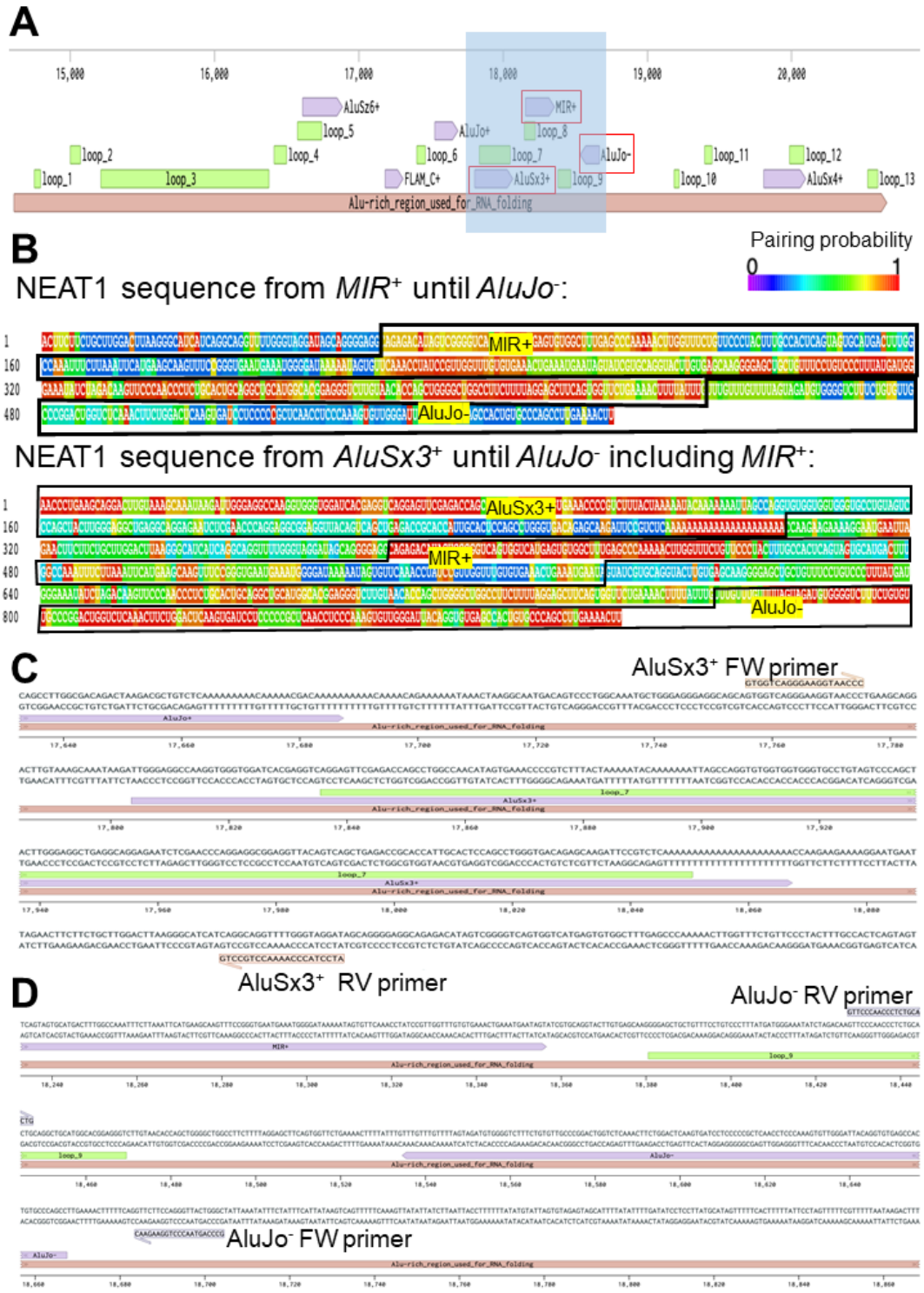

Supplementary Figure 5. A. Graphical representation of the short interspersed nuclear elements in *NEAT1* 3' end and the predicted RNA loops formed. **B.** Base pairing probability of *MIR*$^{+}$/*AluJo*$^{-}$ (upper panel) and *AluSx3*$^{+}$/*MIR*$^{+}$/*AluJo*$^{-}$ (lower panel). **C,D.** Graphical representation of the cDNA region amplified by *AluSx3*$^{+}$ and *AluJo*$^{-}$ primer pairs used for RNA editing studies.

Supplementary Figure 6

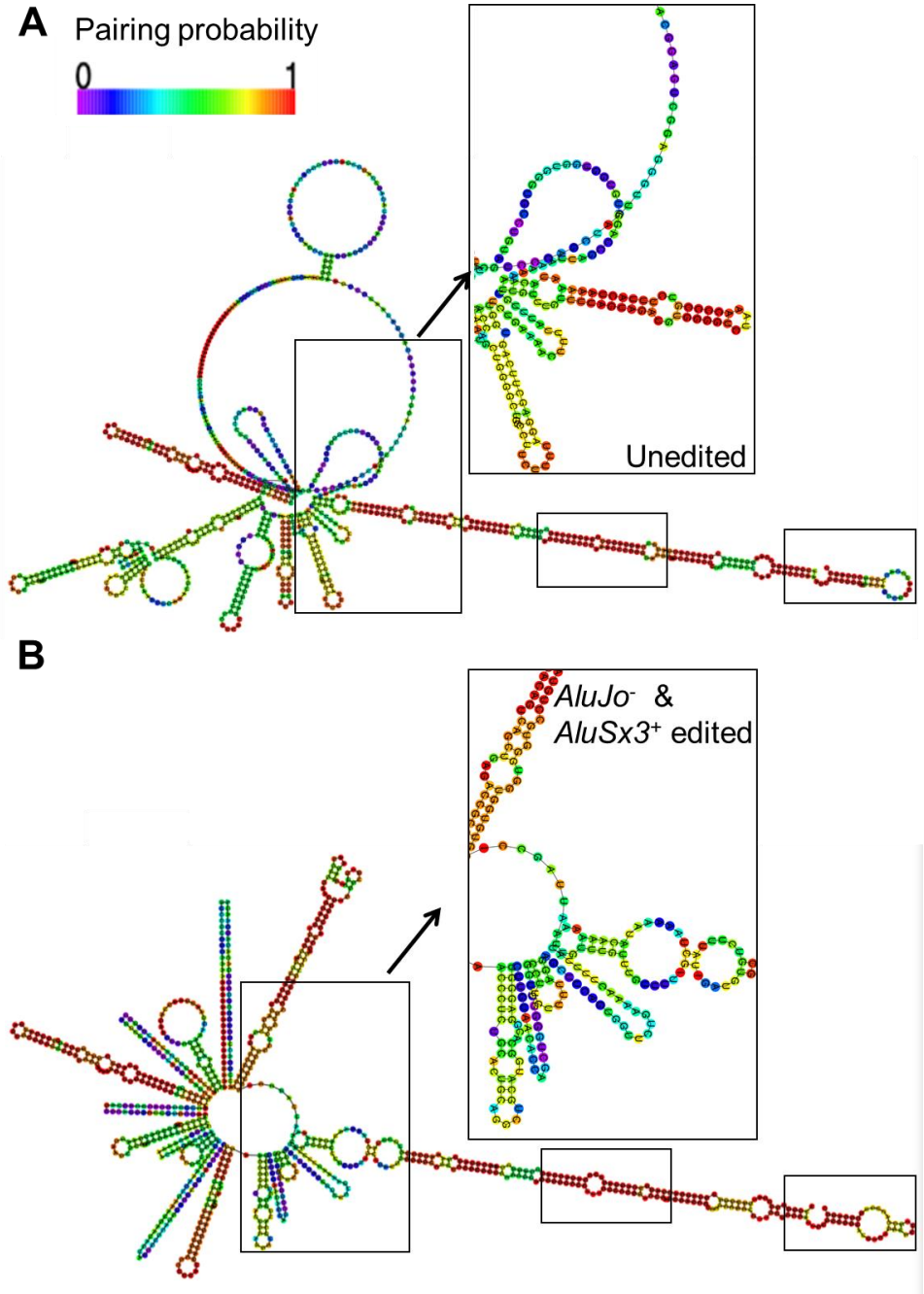

Supplementary Figure 6. A. Graphical representation of NEAT1 3' end depicting Alu elements and AUF1/ HuR binding motifs. **B.** RNA foldback analysis of the region in *NEAT1* 3' end including *AluSx3*$^{+}$*/MIR*$^{+}$*/AluJo*$^{-}$ including all editing sites validated by Sanger-sequencing in our study. The enlarged regions were used in Figure 6C for the mapping of the ARE sites.